

Roles of Activated Carbon and Tetrahydrofuran on Methane Hydrate Phase Equilibrium

Atsadawuth Siangsai^a, Pramoch Rangsunvigit^{*a}, Boonyarach Kitiyanan^a,
Santi Kulprathipanja^b

^aThe Petroleum and Petrochemical College, Chulalongkorn University, Patumwan, 10330 Bangkok, Thailand

^bUOP, A Honeywell Company, Des Plaines, IL 60017, USA

pramoch.r@chula.ac.th

This work studied the effects of activated carbon and tetrahydrofuran (5.56 mol % THF) on methane hydrate phase equilibrium and hydrate dissociation. The hydrate formation was carried out in the quiescent condition and close system at 4 °C. After completion of hydrate formation, the hydrate dissociation was observed by thermal stimulation. The pressure was adjusted to the desired experimental pressure, and then the temperature was increased. When the temperature and pressure in the system crosses the phase boundary, methane gas will release. The results showed that the presence of activated carbon in the system had no effect on hydrate phase boundary, while 5.56 mol % THF affected the thermodynamic methane hydrate phase boundary. Moreover, it indicated that the rate of released gas depended on the experimental pressure, and the methane recovery was in the ranges of 70.0 - 94.9 % in all experiments.

1. Introduction

Natural gas hydrates are occurring naturally form in the marine sediment and permafrost regions. It is a solid crystalline composed of water and gas that formed a cage-like structure or clathrate at the specific temperature and pressure. Natural gas hydrate, mainly methane, is considered to be a potential energy resource (Kim et al., 2011). It is estimated that 44,000 m³ of the world natural gas hydrate reserved found in hydrate (Loh et al., 2012). Interestingly, only 15 % of the potential reserved of natural gas hydrate can provide the world energy at least 200 years at the current energy consumption (Babu et al., 2013). Natural gas in the hydrate form is not only important for the energy resource but also a means for transportation and gas storage (Sloan 2003). For example, Seo et al., 2013 investigated the methane replacement in gas hydrates by carbon dioxide for the methane production and carbon dioxide storage. They revealed that the replacement of methane by carbon dioxide is favoured through the thermodynamic equilibrium. The important property of hydrate is the phase boundary, which separates the region of the stable hydrate form and the region, in which it will be dissociated to water and gas. Accurate phase boundaries of the hydrate are important in the hydrate formation and dissociation experiments or even for the natural gas production from the hydrates and gas separation (Lee and Kang 2013).

The laboratory experiments of methane hydrate formation and dissociation process have been carried out. Linga et al. (2009a) studied the hydrate formation in the water saturated silica sand matrix at 8.0 MPa and 4.0 °C. They observed the hydrate nucleation at multiple locations in the reactor and more than 70 % of water converted to the hydrate for all the hydrate formation experiments. Jin et al. (2012) studied the growth of hydrate in water-unconsolidated sand particles. They reported that the nature of the hydrate in the pores changes during the hydrate growth. Park and Kim (2010) and Kim et al. (2011) demonstrated that the formation rate of methane hydrate increased in the presence of multi-walled carbon nanotubes (MWCNTs), which affected the thermodynamic phase equilibrium of the methane hydrate formation. Tang et al. (2005) reported that the rate of hydrate dissociation increased with the increase in the temperature. Linga et al. (2009b) investigated the methane recovery from the hydrate formed in variable volume bed of silica sand. They reported the two-stage hydrate dissociation and the rate of released methane depended on the bed size of silica sand. Therefore, the objective of this study was to investigate the roles of hydrate

promoter such as activated carbon and tetrahydrofuran (THF) on the hydrate phase equilibrium. In addition, the effects of the promoters on the methane hydrate dissociation were observed.

2. Experimental procedure

2.1 Materials and apparatus

The schematic diagram of gas hydrate apparatus is shown in Figure 1a. It consisted of a high-pressure stainless steel crystallizer (CR) with an internal volume of 57.28 cm^3 and a reservoir (R) with a volume of 50 cm^3 . The crystallizer and reservoir were immersed in a cooling bath, the temperature of which was controlled by an external controllable circulator. The pressure transducers were employed to measure the pressure with 0.13% global error (0-21 MPa). The temperature of the hydrate and gas phases in the crystallizer was measured using k-type thermocouples. Figure 1b shows the cross-section of the crystallizer, where the thermocouples were located at different positions: T1 at the top of the bed, T2 at the middle of the bed, T3 at the bottom of the bed, and T4 at the bottom of the crystallizer. A data logger was connected to a computer to record pressure and temperature during the experiment. Ultra high purity methane (99.999 %, Labgaz Thailand Co., Ltd.) was used in all experiments. Methane hydrate formation and dissociation were observed by adding granular activated carbon (AC), which was supported by Carbokarn Co., Ltd., Thailand ($400\text{-}841 \mu\text{m}$) with the surface area (S_{BET}) and total pore volume of $907 \text{ m}^2/\text{g}$ and $0.55 \text{ cm}^3/\text{g}$, respectively. Tetrahydrofuran (THF, 99.8 %, Lab-Scan, Thailand) was also used as a hydrate promoter for the methane hydrate formation experiment. The THF concentration of 5.56 mol%, was reported to be the most effective hydrate promoter (Lim et al., 2013).

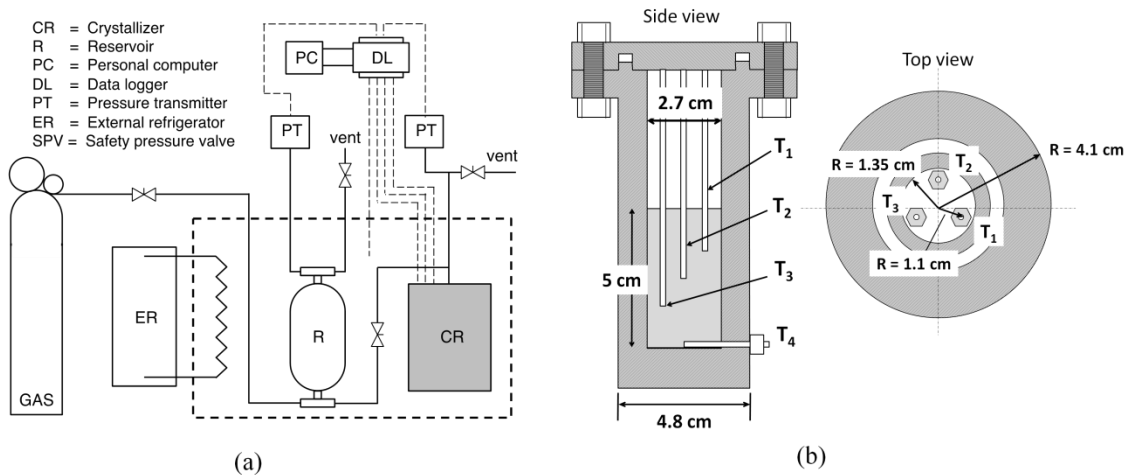


Figure 1: Schematic diagram of gas hydrate apparatus; a) schematic diagram, b) cross-section of a crystallizer

2.2 Procedure

2.2.1. Hydrate formation experiment. The experimental procedure for the hydrate formation in the presence of activated carbon and THF is described elsewhere (Linga et al., 2007). Briefly, the experiment conducted with approximately 13 g of activated carbon (AC), which was fully adsorbed by water and placed in the crystallizer. For THF solution, 30 mL of 5.56 mol % THF was added into the crystallizer. The apparatus was pressurized to 0.5 MPa and depressurized to atmospheric pressure twice to eliminate the presence of air or moisture. The temperature was set to $4 \text{ }^\circ\text{C}$ and maintained by the controllable circulator. The crystallizer was pressurized to a desired experiment pressure. The data was then recorded every 10 s. All hydrate formation experiments were carried out in the quiescent condition with a fixed amount of water and gas in the closed system. The experiment was allowed to continue until no significant change in the pressure. Finally, the pressure and temperature data were used to calculate for the methane consumption (gas uptake).

2.2.2. Hydrate dissociation experiment. After completion of methane hydrate formation, the hydrate was dissociated by thermal stimulation. The pressure in the crystallizer was reduced carefully to the desired pressure, at which the equilibrium temperature was determined by venting out the free gas in the system. Then, the temperature was increased from the formation temperature at the same heating rate for all experiments. This point was marked as time zero for the dissociation experiment. The hydrate dissociates

when the temperature in crystallizer crosses the equilibrium phase boundary, which corresponds to the desired experimental pressure. At any given time, the total number of moles ($n_{T,t}$) in the system remains constant and equal to that at time zero ($n_{T,0}$). Therefore, the mole of released methane from the hydrate at any time during the hydrate dissociation was calculated by Eq(1);

$$\Delta n_{H,\uparrow} = n_{H,0} - n_{H,t} = \left(\frac{PV}{zRT} \right)_{G,t} - \left(\frac{PV}{zRT} \right)_{G,0} \quad (1)$$

(1) where z is the compressibility factor calculated by Pitzer's correlation (Veluswamy and Linga, 2013). R is the universal gas constant. V is the volume of gas phase in the crystallizer. P and T are the pressure and temperature of the crystallizer. $\Delta n_{H,\uparrow}$ is the mole of gas released from the hydrate. $n_{H,0}$ is the mole of gas at time zero. $n_{H,t}$ is the mole of the gas at time t . Subscripts of $G,0$ and G,t represent the gas phase at time zero and time t , respectively. The methane recovery was calculated by Eq(2) as a function of time for any dissociation experiment based on its information of formation experiment.

$$\% \text{methane recovery} = \frac{(\Delta n_{H,\uparrow})_t}{(\Delta n_{H,\downarrow})_{t_{\text{End}}}} \times 100 \quad (2)$$

where $(\Delta n_{H,\downarrow})_{t_{\text{End}}}$ is the mole of consumed gas for the hydrate formation at the end of experiment. $(\Delta n_{H,\uparrow})_t$ is the mole of released gas from the hydrate during the hydrate dissociation at any given time.

3. Results and discussion

3.1 Methane recovery

Table 1 shows the hydrate dissociation experiment conditions. There are two systems in the experiment, including AC/methane/water and 5.56 mol % THF/methane. As seen from the system of AC/methane/water, the CH_4 recovery is between 70.0 - 94.9 % for the experiments performed at 7.0 and 5.3 MPa. The dissociation temperatures (T_d) of experiments conducted at 7.0 MPa and 5.3 MPa are around 9 and 6 °C. The dissociation temperature is also based on the hydrate phase boundary. The rates of released methane of the system conducted with AC/water/methane is increased when increasing the experimental pressure as same as the result of conducted 5.56 mol % THF/methane system.

For the system of 5.56 mol % THF/methane, the experiments were performed at the experimental pressure of 6.5 and 4.6 MPa. The dissociation temperature was significantly increased from the system of AC/water/methane, and also increased with the increased pressure. This indicates that the presence of THF in the system changes the phase boundary of the methane hydrate to a higher temperature, which was discussed in section 3.2. Moreover, the methane recovery is 79.3 - 85.1 %. There are small amount of methane gas that dissolved during the formation experiment remains in the liquid phase and is not recoverable.

Table 1: Hydrate dissociation experiment conditions

Exp. No.	Experimental pressure, P_{exp} (MPa)	ΔT^a (°C)	T_d at P_{exp}^b (°C)	Rate of released methane (mol/h) (R^2 value)	CH_4 recovery (mol%)
AC/water/methane					
1	7.0	13	9.5	0.1287(0.9957)	94.9
2	7.0	13	9.2	0.1171(0.9864)	80.7
3	5.3	13	6.6	0.0898(0.9966)	91.7
4	5.3	13	6.4	0.0615(0.9913)	70.0
5.56 mol % THF/methane					
5	6.5	29	27.7	0.3148(0.9889)	82.5
6	6.5	29	27.1	0.3363(0.9903)	79.3
7	4.6	29	24.9	0.0735(0.9894)	87.4
8	4.6	29	25.1	0.0950(0.9944)	85.1

^a $\Delta T = T_{\text{End}} - T_{\text{Start}}$

^b T_d = The dissociation temperature at which methane released from the hydrate for the experiment pressure, P_{exp}

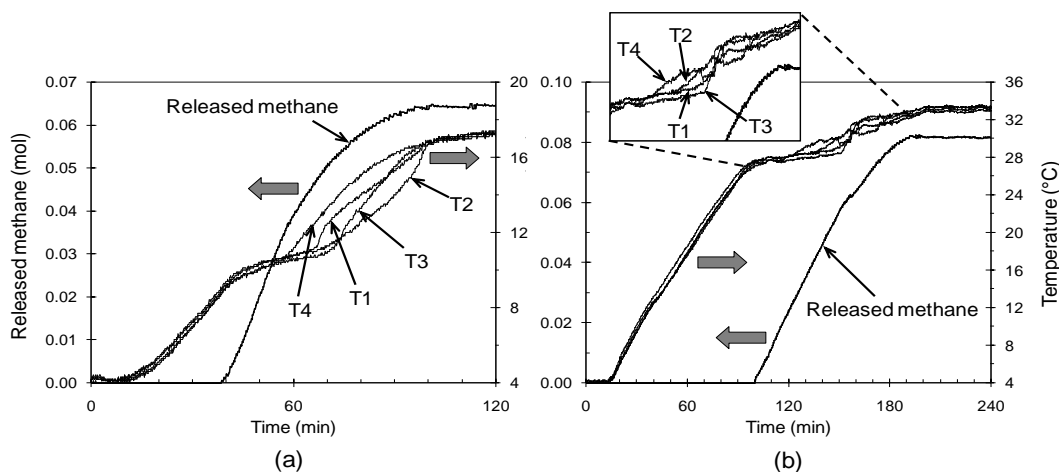


Figure 2: Typical released methane and temperature profiles of hydrate dissociation; a) AC/water/methane (Experiment 1, Table 1) and b) 5.56 mol% THF/methane (Experiment 6, Table 1)

Figures 2a and 2b present the typical released methane and temperature profiles of hydrate dissociation from the systems with activated carbon and 5.56 mol% THF (Experiments 1 and 6, Table 1). After the hydrate formation completion, the pressure in the crystallizer was reduced to a desired pressure, and the temperature in the system was increased to recover the gas from the hydrate. As seen in Figure 2a, the change in temperature profiles, caused by the balance of heat transfers between external heater and methane hydrate dissociation (endothermic process), indicate the first released methane point at around 9.5 °C, which is marked as the dissociation temperature. Then, the amount of methane gas obviously increases until it reaches the plateau. Moreover, the four thermocouples were placed at different positions to detect the methane hydrate dissociation regions. It can be noticed that all methane hydrate regions begin to dissociate at the same temperature and time, as seen in the figure. However, the thermocouple at T4 increases firstly followed by T1, while T2 and T3 are still in the line, indicating that the methane hydrate in each region could take different time to finish the dissociation. The dissociation completes when the temperatures of all thermocouples reach the set point.

The released methane and temperature profiles of the hydrate dissociation from 5.56 mol% THF/methane in Figure 2b show almost the same results as in the system of AC/water/methane. The difference is the dissociation temperature of this system is higher than that of AC/water/methane. In addition, there is a two-stage dissociation, which is caused by the dissociation in different regions of the hydrate in the crystallizer, detected by the thermocouples in the different locations. Generally, hydrate dissociation occurs randomly in different regions after thermal stimulation. In our experiment, we performed the hydrate dissociation experiment in a small crystallizer. In this case, the dissociation cannot be clearly observed by the thermocouples. But, in the case of a large crystallizer, the dissociation is clearly present (Linga et al., 2009b).

3.2 Hydrate phase equilibrium

Figure 3 shows the phase equilibrium points of experiments conducted with activated carbon and 5.56 mol % THF. The equilibrium points of the experiment with the presence of activated carbon fit quite well with the methane hydrate phase equilibrium curve in the system with only water reported by Zanota et al. (2005). The results of phase equilibrium of AC/water/methane system indicates that the activated carbon does not affect the methane hydrate phase equilibrium. This is because the activated carbon or even other porous medias do not change the thermodynamic of the water-methane hydrate system. The roles of adding the porous media in the system is only to increase the contact area between the gas phase and water phase in the system resulting in reducing the hydrate formation time and increasing the amount of gas consumption (Linga et al., 2009a), which was recently confirmed (Babu et al., 2013). On the contrary, 5.56 mol % THF significantly affects the thermodynamic of methane hydrate phase equilibrium by changing the properties of the liquid phase in the system. Hence, the hydrate phase equilibrium changes with the presence of THF, as seen from Figure 3. Similarly, Lirio and Pessoa (2013) also observed that THF can shift the phase equilibrium curve of carbon dioxide hydrate to the more stable region. There are several independent equilibrium points in agreement with the phase boundary reported by Lim et al., (2013). The roles of hydrate promoter in this study, activated carbon and THF, are important for the gas separation, gas storage, gas transportation or event the gas production from the hydrates.

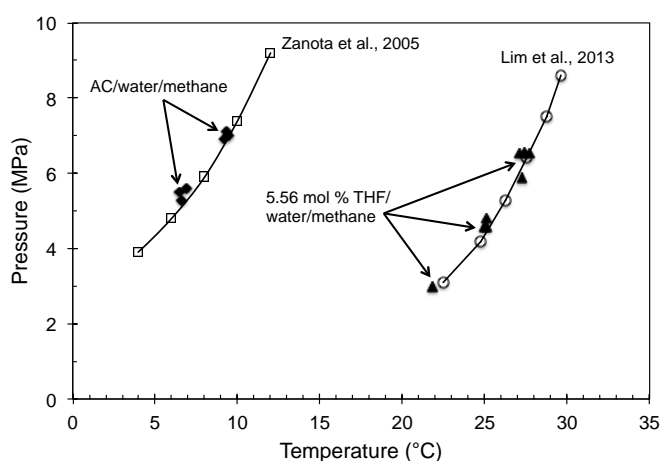


Figure 3: Comparison of phase equilibrium

4. Conclusion

This work investigated the effects of activated carbon and tetrahydrofuran (THF) on methane hydrate phase boundary. The methane recovery from the hydrate was also studied by thermal stimulation. The results showed that the presence of THF with the concentration of 5.56 mol % affected the thermodynamic of methane hydrate phase equilibrium by increasing the equilibrium temperature at a given experimental pressure, while the presence of activated carbon had no effect on the hydrate phase equilibrium. However, the activated carbon increased the rate of methane hydrate formation compared to the system without. Moreover, the rate of released methane during the hydrate dissociation depended on the experimental pressure. In other words, at the high experimental pressure, methane was released faster than that at the low pressure. The methane recovery was in the range of 70.0 -94.9 % in all experiments.

Acknowledgement

This work was supported by The Golden Jubilee Ph.D. Program (2.P.CU/51/J.1), Thailand Research Fund; The Petroleum and Petrochemical College (PPC), Chulalongkorn University, Thailand; National Metal and Materials Technology Center (MTEC), Thailand; Center of Excellence on Petrochemical and Materials Technology (PETROMAT), Thailand; Ratchadaphiseksomphot Endowment Fund of Chulalongkorn University (RES560530021-CC); and UOP, A Honeywell Company, USA.

References

- Babu P., Yee D., Linga P., Palmer A., Khoo B.C., Tan T.S., Rangsunvigit P., 2013, Morphology of methane hydrate formation in porous media, *Energy and Fuels*, 27, 3364-3372.
- Jin Y., Konno Y., Nagao J., 2012, Growth of methane clathrate hydrates in porous media, *Energy and Fuels*, 26, 2242-2247.
- Kim N.J., Park S.S., Kim H.T., Chun W., 2011, A comparative study on enhanced formation of methane hydrate using CM-95 and CM-100 MWCNTs, *International Communications in Heat and Mass Transfer*, 38, 31-36.
- Lee J.W., Kang S.P., 2013, Formation behaviours of mixed gas hydrates including olefin compounds, *Chemical Engineering Transactions*, 32, 1921-1926. DOI: 10.3303/CET1332321.
- Lim S.H., Riffat S.B., Park S.S., Oh S.J., Chun W., Kim N.J., 2013, Enhancement of methane hydrate formation using a mixture of tetrahydrofuran and oxidized multi-wall carbon nanotubes. *International Journal of Energy Research*, 38, 374-379.
- Linga P., Haligva C., Nam S.C., Ripmeester J.A., Englezos P., 2009a, Gas hydrate formation in a variable volume bed of silica sand particles, *Energy and Fuels*, 23, 5496-5507.
- Linga P., Haligva C., Nam S.C., Ripmeester J.A., Englezos P., 2009b, Recovery of methane from hydrate formed in a variable volume bed of silica sand particles, *Energy and Fuels*, 23, 5508-5516.

- Linga P., Kumar R., Englezos P., 2007, Gas hydrate formation from hydrogen/carbon dioxide and nitrogen/carbon dioxide gas mixtures, *Chemical Engineering Science*, 62, 4268-4276.
- Lirio C.F.S., Pessoa F.L., 2013, Enthalpy of dissociation of simple and mixed carbon dioxide clathrate hydrate, *Chemical Engineering Transactions*, 32, 577-582. DOI: 10.3303/CET1332097.
- Loh M., Falser S., Babu P., Linga P., Palmer A., Tan T.S., 2012, Dissociation of fresh- And seawater hydrates along the phase boundaries between 2.3 and 17 MPa, *Energy and Fuels*, 26, 6240-6246.
- Park S.S., Kim N.J., 2010, Multi-walled carbon nanotubes effects for methane hydrate formation, *Proceeding in The 2nd International Conference on Computer and Automation Engineering (ICCAE)*, 5, 294-297.
- Seo Y., Lee S., Lee J., 2013, Experimental verification of methane replacement in gas hydrates by carbon dioxide, *Chemical Engineering Transactions*, 32, 163-168. DOI: 10.3303/CET1332028.
- Sloan E.D., 2003, Fundamental principles and applications of natural gas hydrates, *Nature*, 426, 353-359.
- Tang L.G., Xiao R., Huang C., Feng Z.P., Fan S.S., 2005, Experimental investigation of production behavior of gas hydrate under thermal stimulation in unconsolidated sediment, *Energy and Fuels*, 19, 2402-2407.
- Veluswamy H.P., Linga P., 2013, Macroscopic kinetics of hydrate formation of mixed hydrates of hydrogen/tetrahydrofuran for hydrogen storage, *International Journal of Hydrogen Energy*, 38, 4587-4596.
- Zanota M.L., Perier-Camby L., Chuavy F., Brullé Y., Herri J.M., 2005, Improvement of methane storage in activated carbon using methane hydrate, *Proceeding in the Fifth International Conference on Gas Hydrates (ICGH5)*, Trondheim, Norway